



Montréal, Québec
May 29 to June 1, 2013 / 29 mai au 1 juin 2013

The Effect of Subduction and Crustal Ground Motions on the Behaviour of Low-rise CBF Buildings in Victoria BC

Aid Jnaid¹, Lucia Tirca¹ and Ashutosh Bagchi¹

¹Department of Building, Civil and Environmental Engineering, Concordia University, Montreal, Quebec

Abstract: The aim of this paper is a study on the seismic behaviour of a 4-storey moderately ductile Concentrically Braced Frame (CBF) building located on firm soil in Victoria, BC. The nonlinear analysis of the CBF building was carried out using the OpenSees framework and the investigated parameters were: interstorey drift, residual interstorey drift, and the type of failure mode. Nonlinear beam-column elements with spread plasticity and fiber cross-sections were used to model the behaviour of braces. In this simulation, the fracture of braces was considered by assigning the fatigue material model proposed by Uriz (2005). The building was subjected to both crustal and subduction ground motions. The results show that braces experienced large demand at the ground floor level and developed large deformation in tension after the occurrence of buckling in compression.

1 Introduction

Concentrically brace frames (CBF) are widely used in North America and are designed to resist gravity, wind, and earthquake loads in agreement with the current code and standard provisions. By following the conventional design criteria, braces are prone to unsymmetrical hysteresis in tension and compression, while the distribution of the internal forces and deformations is strongly influenced by the frequency contents of ground motions. Notwithstanding their robust stiffness, CBFs are prone to concentrate the lateral forces and deformations within a floor that consequently leads to the formation of a soft storey mechanism.

Buildings designed in western Canada, (e.g. Victoria, BC) are prone to crustal and Cascadia subduction ground motions. Recent investigations have revealed that the distance to the fault of Victoria, Vancouver and Seattle is less than 120 km (Atkinson and Macias, 2009). The Cascadia subduction thrust-fault mechanism is due to the landward and beneath to the continent movement of the Juan de Fuca plate at an average speed of 40 mm/year (Earthquakes Canada, 2012). On the west-east axis, Juan de Fuca plate lies between the Pacific plate and the North American plate, while on the north-south axis it lies between the Vancouver Island and northern California. The Cascadia thrust fault produces rare and large magnitude earthquakes that may reach a magnitude of M9 and the epicentre may occur on the vicinity of Seattle – Victoria axis. The recurrence period for a Cascadia subduction earthquake is approximately 500 years. Likewise for the magnitude M9 Japan Tohoku earthquake (Ghofrani et al, 2012), Cascadia records are estimated to be characterized by long duration and high frequency content.

The purpose of this paper is to investigate the behaviour of a low-rise concentrically braced frame building located on firm soil in Victoria, BC., when subjected to a set of crustal and subduction ground motions, likely Tohoku records.

2 Building description

2.1 Building geometry

The building design is conducted according to the CSA/S16-2009 standard in conjunction with the requirements of the National building code of Canada (NBC 2010). The plan view and the CBF elevation located in gridline 2 is shown in Figure 1. In the east-west direction, the building is braced with four CBFs in chevron bracing configuration. In this study, only the two identical CBFs located in the north-south direction are investigated. At the roof level, the dead load is 3.8 kPa and at the typical floor is 4.4 kPa. The live load for the typical floor is 2.4 kPa and the snow load is 1.08 kPa. For cladding, 1.0 kPa was considered.

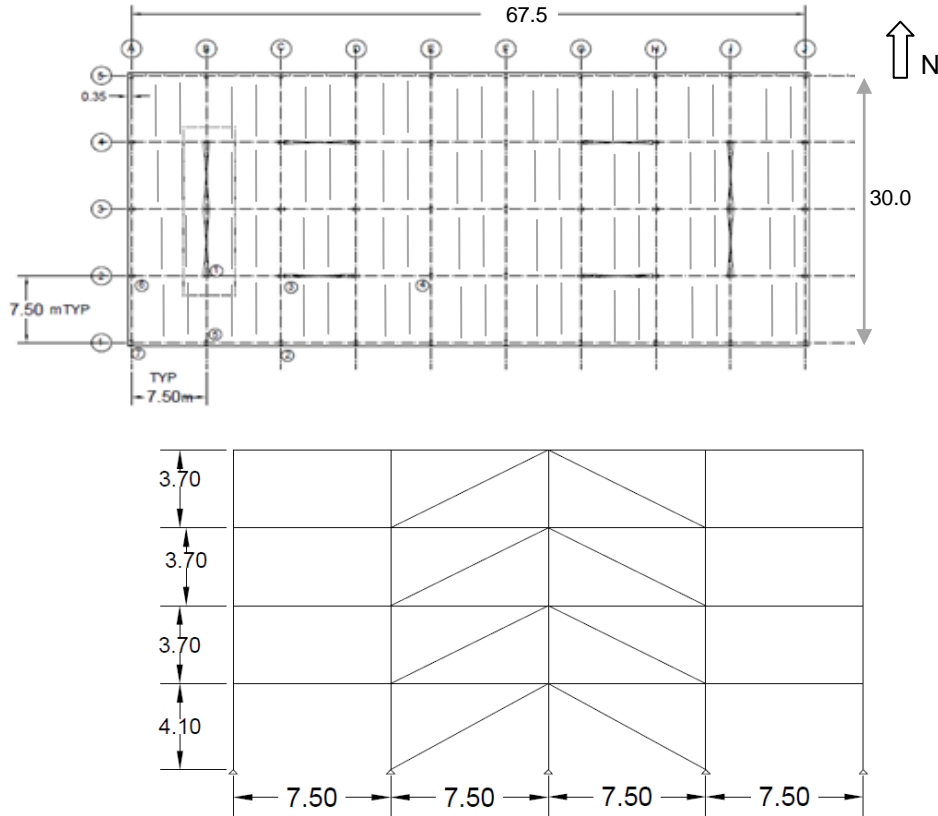


Figure 1: Building plan and elevation.

According to the NBCC 2010, the seismic base shear is computed as:

$$V = \frac{S(T_a)M_v I_E W}{R_d R_0} \quad (1)$$

where $S(T_a)$ is the design spectral acceleration corresponding to the fundamental period of the building, which is estimated as $T_a = 0.025h_n$ and h_n is the building height. Herein, M_v is the higher mode factor, I_E is the importance factor, R_d is the ductility-related force modification factor and R_0 is the overstrength-related force modification factor. The 4-storey office building is located on a firm soil in Victoria, B.C. and is classified as normal importance category. The spectral acceleration values for Victoria at the period of 0.2, 0.5, 1.0 and 2.0 s are equal to 1.2, 0.82, 0.38 and 0.18 g, respectively. In this study, the CBF systems were considered moderately ductile with $R_d = 3$ and $R_0 = 1.3$. The value of the computed base shear V should not be larger than the maximum base shear given by the following equation: $V_{max} = 2/3[S(0.2)M_v I_E W / R_d R_0]$. For verifying the torsional sensitivity of the building structure, the parameter $B_x =$

$\delta_{ave}/\delta_{max}$ was calculated in agreement with the NBC 2010 provisions, where δ_{ave} and δ_{max} are the average displacement and the maximum displacement of the structure at level x , respectively. Herein, B_x is the ratio at level x used to determine the torsional sensitivity and in this example, for all storeys, the values of B_x were found to be lower than 1.7. Thus, the studied building was considered to be regular.

The design of CBF members was conducted in accordance with the CSA/S16-2009 standard and all members are made of steel with $F_y = 350$ MPa. All beams and columns cross-sections are made of W-shape, while braces are made of hollow structural sections, HSS. In addition, all braces, beams and braced bent columns are designed as Class 1 sections, while they are proportioned to carry the seismic load in combination with the gravity load. The designed building should meet the interstory drift limitations of $2.5\%h_s$ as per the NBC 2010 code, where h_s is the storey height. The CBF braces, showed in Figure 1, were preliminary proportioned based on the static equivalent method. Then, the dynamic analysis procedure by the modal response spectrum method was employed and the period of the building in the first two modes, as resulted from the ETABS output, is illustrated in Table 1. Using the results obtained from the response spectrum analysis, the computed members sizes are given in Table 2.

Table 1. The first and second vibration mode period.

	T1(s)	T2(s)
ETABS	0.650	0.242
OpenSees	0.649	0.238

Table 2. Members sizes.

Storey	Braces	Beams	Columns
4	HSS 178x178x9.5	W 360x86	
3	HSS 203x203x13	W 360x91	W 360x91
2	HSS 254x254x13	W 360x110	
1	HSS 254x254x13	W 360x110	W360x162

2.2 Ground motion selection and scaling methodology

The NBC 2010 requires that the selected ground motions should be scaled to match the uniform hazard spectrum for Victoria (UHS) computed as 2% of exceedance in 50 years. When using seven or more ground motions, the ASCE/SEI-7 specifications requires to consider the average response of records, but when only three records are used, the maximum response should be taken. In this study, the methodology of scaling ground records mentioned in ASCE/SEI-7 is used. This methodology requires that the mean of the scaled ground motions should be equal or greater than the UHS over the period of interest $0.2T_1 - 1.5T_1$. In addition, the selected ground motions should be suitable for the type of soil at the building location. For example, the site class C is defined when the average shear wave velocity \bar{V}_s in top 30 m layer is in the range of $360 \text{ m/s} < \bar{V}_s < 760 \text{ m/s}$.

To analyse the behaviour of the low-rise CBF building in Victoria, two sets of ground motions are considered: (i) crustal ground motions, and (ii) subduction ground motions (e.g., Tohoku ground motions). The crustal and subduction records were selected from two ground motions database given in the footnote of Table 3. Records from the K-Net database have been corrected using a linear baseline correction and a Butterworth bandpass filter ($Frequency1 = 0.1$, $Frequency2 = 25$, $Order 4$) (De Luca et al., 2011). The selected ground motions are shown in Table 3 together with the peak ground acceleration, PHA , peak ground velocity, PGV , the PGV/PHA ratio, the total duration, t , the Trifunac duration, t_d , the predominant period of ground motions, T_p , and the main period, T_m . Among the seven crustal ground motions, six have a total duration of 40 s and one has 60 s, while the average value of the Trifunac duration is 11.3 s. The average shear wave velocity of the seven crustal ground motions is 424 m/s with a minimum value of 360 m/s and a maximum value of 489 m/s. The average value of velocity and acceleration of the selected ground motions is 0.28 m/s and 0.33 g, respectively, while the average value

of the predominant and mean period of selected crustal ground motions is: 0.21 s and 0.53 s. In comparison, the selected seven Tohoku ground motions show a large duration of 300 s, while the average of the Trifunac duration is 67 s. This value is six times longer than that of the crustal ground motion set. The average shear wave velocity is in the same range as that computed for the crustal records set, while the average value of velocity and acceleration that corresponds to the selected records of magnitude 9 Tohoku earthquake is larger: 0.39 m/s and 0.8 g, respectively. However, Tohoku records are characterized by high frequency with an average T_p value of 0.25 s and an average T_m value of 0.19 s. In comparison with the crustal records, the predominant periods of the Tohoku records are in the same range, while the mean period is about three times lower. At the same time, some Tohoku records are characterized by a combination of two wave shapes arising from the propagation of rupture along the shore, while following a north – south axis. In this light, the S1, S2, S3 records show a double pulse wave, while the others are characterized by a single wave similar to crustal records. The scaling factor computed to match the UHS in the $0.2T_1 - 1.5T_1$ interval is given in Table 4. The procedure used for scaling is that proposed by Reyes and Kalkan (2012). The acceleration response spectrum of the scaled crustal and subduction records are illustrated in Figure 2 together with the average value and the UHS as required by NBC 2010 for Victoria, soil class C.

Table 3. Characteristics of selected ground motions.

No	Event	MW	Station	$R_{hyp}^{3)}$ (km)	Com ($^{\circ}$)	PHA (g)	PHV (m/s)	PHV/ PHA (s)	t (t_d) (s)	T_p (T_m) (s)
Subduction ground motions ¹⁾										
S1	2011/11/3 Tohoku	9	MYG001	155	EW	0.43	0.23	0.055	300 (83)	0.27 (0.26)
S2	2011/11/3 Tohoku	9	MYG004	184	EW	1.22	0.48	0.041	300 (85)	0.26 (0.25)
S3	2011/11/3 Tohoku	9	FKS005	175	EW	0.45	0.35	0.084	300 (92)	0.32 (0.15)
S4	2011/11/3 Tohoku	9	FKS010	189	EW	0.86	0.56	0.066	300 (66)	0.27 (0.18)
S5	2011/11/3 Tohoku	9	FKS009	216	EW	0.83	0.44	0.054	300 (74)	0.20 (0.20)
S6	2011/11/3 Tohoku	9	IBR004	273	EW	1.03	0.38	0.038	300 (33)	0.21 (0.15)
S7	2011/11/3 Tohoku	9	IBR006	283	EW	0.78	0.3	0.039	300 (36)	0.25 (0.12)
Crustal ground motions ²⁾										
C1	Jan. 17, 1994 Northridge	6.7	Castaic, Old Ridge Route	44	90	0.57	0.52	0.09	40 (9.1)	0.26 (0.54)
C2	Jan. 17, 1994 Northridge	6.7	LA - UCLA Grounds	25	90	0.28	0.22	0.08	60 (11.3)	0.22 (0.34)
C3	Jan. 17, 1994 Northridge	6.7	Moorpark - Fire Station	36	180	0.29	0.20	0.07	40 (14.2)	0.26 (0.47)
C4	Oct. 18, 1989 Loma Prieta	6.9	Gilroy Array #3 Palo Alto - SLAC	36	0	0.56	0.36	0.07	40 (6.37)	0.20 (0.37)
C5	Oct. 18, 1989 Loma Prieta	6.9	Lab Apeel 9-Crystal	54	360	0.28	0.29	0.11	40 (11.6)	0.3 (0.65)
C6	Oct. 18, 1989 Loma Prieta	6.9	springs resort Anderson Dam	41	227	0.11	0.18	0.17	40 (16.2)	0.3 (0.88)
C7	Oct. 18, 1989 Loma Prieta	6.9	(Downstream)	20	250	0.25	0.20	0.09	40 (10.4)	0.2 (0.46)

¹⁾ Subduction ground motions were selected from: www.k-net.bosai.go.jp

²⁾ Crustal ground motions were selected from: http://peer.berkeley.edu/peer_ground_motion_database/

³⁾ In this table, only the hypocentral distance is reported, not the distance to the fault.

The acceleration response spectrum obtained from the selected Tohoku records show very large ordinates in the short period range 0.1 - 0.35 s. Thus, low-rise buildings with a fundamental period in this

range may be exposed to ground motions that are two times larger than those required by the code. However, buildings with a fundamental period larger than 1.6 s are not exposed to increased acceleration response spectrum ordinates. Although in the interval of 0.7-0.8 s, the average spectrum shows a slightly lower value than that required by code, the scale factor was not raised above 1.0. On the contrary, the selected crustal records show a drop in the interval 0.0 - 0.15 s.

Table 4. Scaling factors for crustal and subduction GMs for 4-storey building in Victoria.

No.	Record	Scaling factor	No.	Record	Scaling factor
C1	NR 963	1.00	S1	MYG001-EW	1.0
C2	NR1006	1.95	S2	MYG 004-EW	1.0
C3	NR1039	1.90	S3	FKS005-EW	1.0
C4	LP 767	1.00	S4	FKS010-EW	1.0
C5	LP 787	1.20	S5	FKS010-EW	1.0
C6	LP 736	2.60	S6	IBR004-EW	1.0
C7	LP 739	1.90	S7	IBR006-EW	1.0

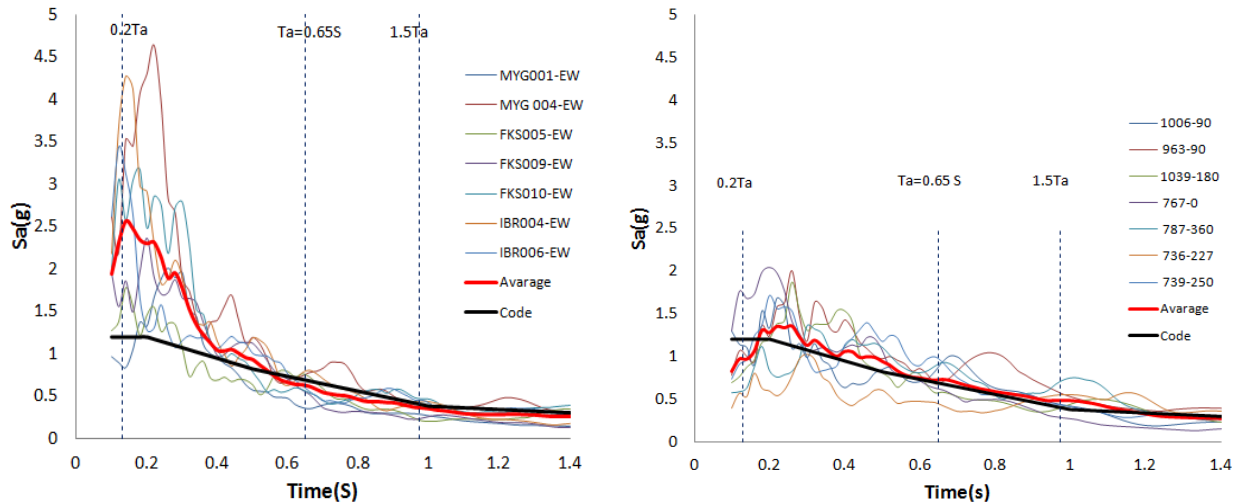


Figure 2. Acceleration response spectrum of scaled ground motions: a) subduction; b) crustal.

3 Numerical modeling

3.1 Structural model

To emphasize the inelastic behaviour of the selected CBF, the OpenSees framework (McKenna et al., 2004) is employed and the nonlinear time-history analysis was used. To model the structure in the OpenSees environment, Steel 02 material (Giuffre-Menegotto-Pinto) with isotropic strain hardening was assigned to all steel members. Due to the symmetry of the building structure, the OpenSees model was built for half of the building as illustrated in Figure 3. The illustrated model accounted for the three-dimensional effect and allowed the deformation of braces in-plane and out-of-plane by assigning an initial camber of $L/500$, where L is the length of the brace. To model the structural members in OpenSees, fiber sections were assigned to all elements (Aguero et al., 2006). Thus, each brace was modeled by using twenty nonlinear beam-column elements with spread plasticity distributed across the member length. In this model, each element was defined with 4 integration points, while the fiber section of the HSS brace cross-section was meshed with round corners and 200 fibers. The beams and columns of braced frame were modeled as beam with hinges elements. Beams were pinned-connected to the columns, while all columns were continuous over two-storeys. Braces were connected to frame by means of gusset plate

connections. The properties of the gusset plate connections were considered by assigning two rotational and one torsional spring in the zero-length element located between each end of the brace member and the rigid link member. The out-of-plane flexural stiffness of the gusset plate, as proposed by Hsiao et al. (2012) is EI/L_{ave} , where L_{ave} is the average of $L1$, $L2$ and $L3$ that are illustrated in Figure 4 and the moment of inertia, I is given by the following equation: $I = B_w t_g^3 / 12$. Herein, B_w is the Whitmore width which is defined by the 30° projection angle, E is the elastic modulus and t_g the thickness of the gusset plate. The out-of-plane plastic bending moment of the gusset plate is ZF_y where $Z = B_w t_g^2 / 4$ is the plastic section modulus. The in-plane flexural stiffness of the gusset plate should be larger than that of the attached brace member. A third torsional spring is assigned in the zero-length element in order to consider the torsional stiffness of the gusset plate defined as GJ/L_{ave} where G is the shear modulus of steel and J is the torsional constant given by: $J = 0.333B_w t_g^3$. Based on experimental tests, the failure mode of a brace was found to be fracture of the brace at its mid-span where the plastic hinge formed. The fracture mechanism is due to low-cycle fatigue when cracks are formed and propagate after the occurrence of local buckling. To simulate the effect of low-cycle fatigue, Uriz (2005) proposed and developed in OpenSees the fatigue material model. This material is wrapped around the parental material Steel-02. Uriz has calibrated the fatigue material and defined the material constants $\epsilon_0 = 0.095$ and $m = 0.5$. The 2% Rayleigh damping, referred to as mass- and stiffness-proportional damping, was assigned to the first and third mode of vibration.

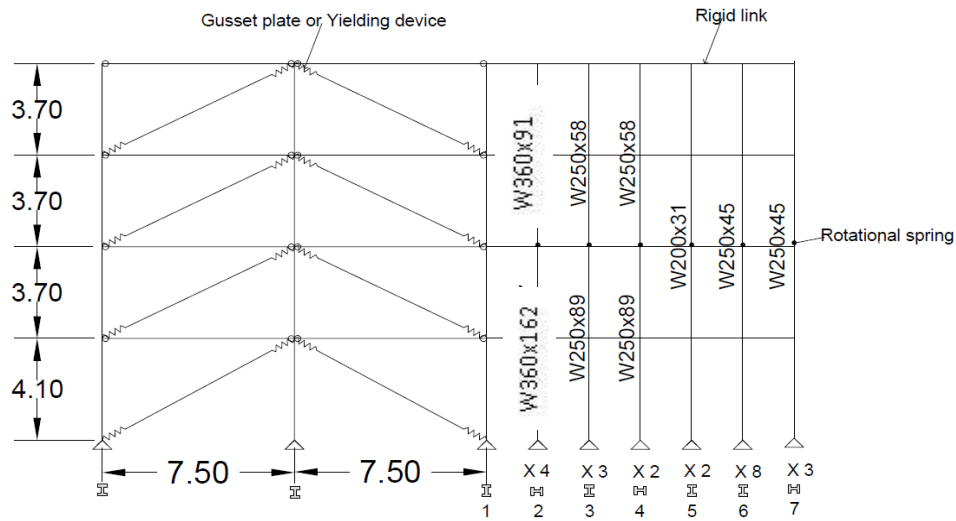


Figure 3. OpenSees model.

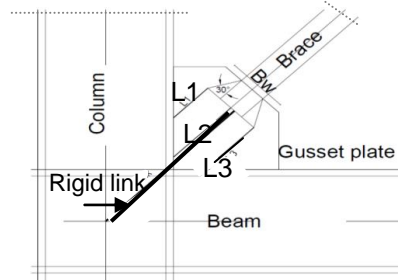


Figure 4. Brace-to-frame connection model.

3.2 Numerical results

The nonlinear response of the 4-storey building designed for Victoria, BC is presented in terms of the building deformation. It was observed that in all cases, the demand was larger at the ground floor level where braces experienced buckling and yielding, while braces located at the upper floors responded in the elastic range. To illustrate this behaviour, the interstorey drift across the building height is plotted in

Figure 5 for all 14 ground motions together with the mean and the 84 fractile (84%)s. The interstorey drift is expressed in % h_s . The seismic response under the C1 and C2 records is shown in Figure 6.

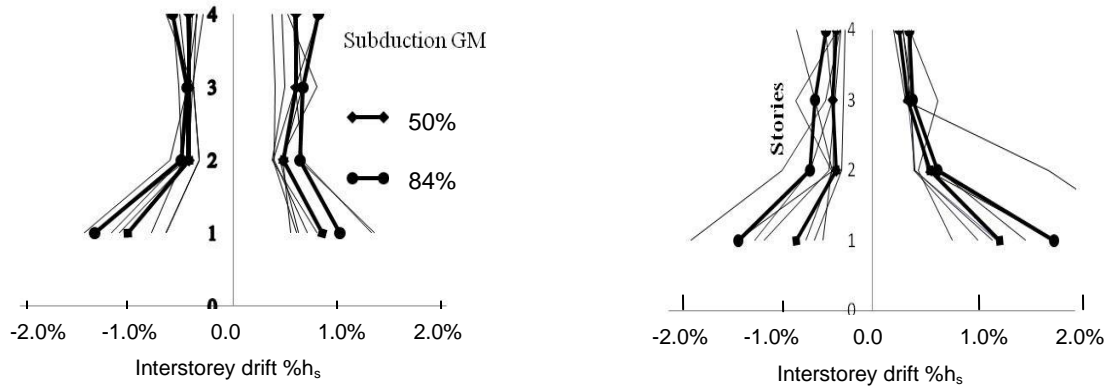


Figure 5. Interstorey drift of the 4-storey CBF building: a) subduction GM; b) crustal GM.

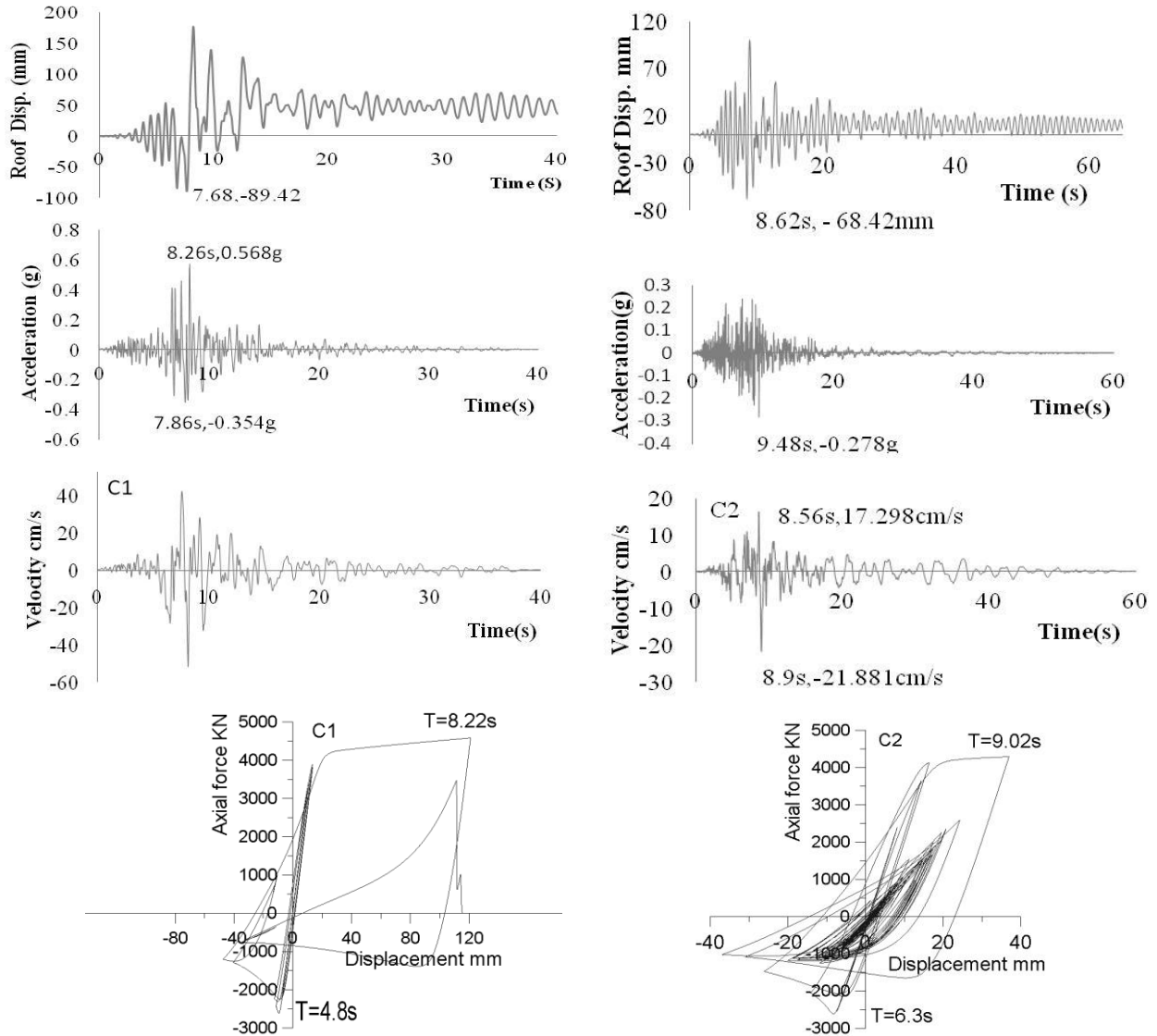


Figure 6. Seismic response of the 4-storey CBF building under the C1 and C2 ground motions.

As depicted in Figure 5, the subduction ground motions set illustrates a maximum interstorey drift at the ground floor level around $1.4\%h_s$, while at all floor it is below $0.8\%h_s$. The set of crustal ground motions imposes the development of a larger interstorey drift at the ground floor level that may reach $2.0\%h_s$. However, the interstorey drift is within the code limit of $2.5\%h_s$. It seems that the building deformation is concentrated within a floor (in this case ground floor level) and may lead to the development of a storey mechanism. In this light, Figure 6 illustrates the time-history displacement recorded at the roof level that resulted under the crustal ground motions. The accelerogram and velocity time-series are plotted as well. From Figure 6, it is observed that a large residual roof displacement of about 50 mm was developed under the input of C1 ground motion. In both illustrated cases, braces located at the ground floor level were subjected to yielding in tension after buckling in compression. Under the C1 record, one of the two ground floor braces experienced tensile fracture. The response under the crustal ground motions C5 and C7 is illustrated in Figure 7. Under both C5 and C7 ground motions, there is no residual roof displacement, although the braces at the ground floor level were subjected to buckling in compression and yielding in tension. In this case, braces belonging to the upper floor levels performed almost elastically.

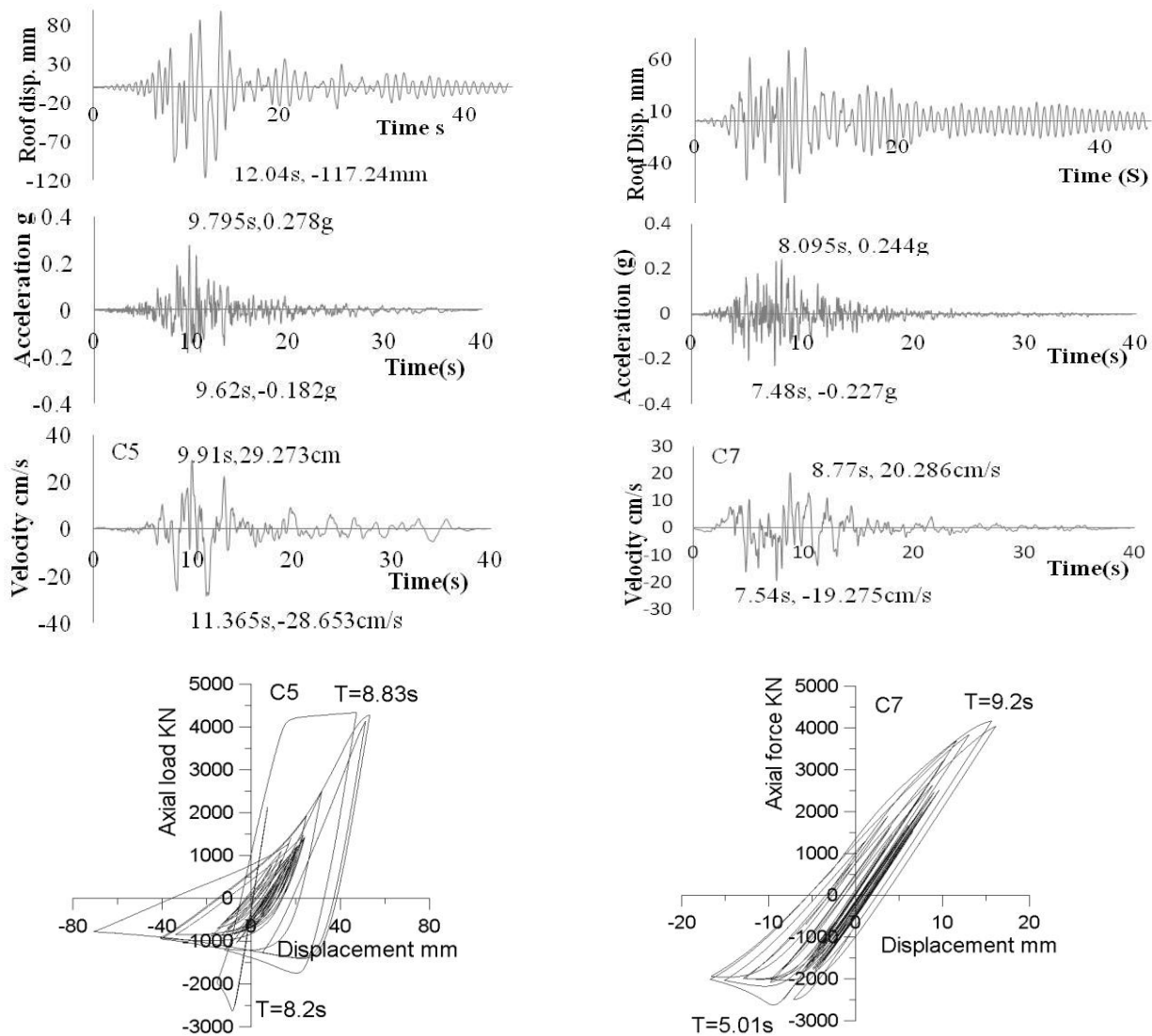


Figure 7. Seismic response of the 4-storey CBF building under the C5 and C7 ground motions.

The response of the building under the subduction ground motions S2, S3 and S7 is illustrated in Figure 8. The three records show different accelerogram types. Thus, the S2 and S3 ground motions show a

combination of two seismic waves that arrived at about 20 s interval, while the S7 illustrates the record of a single wave. As depicted bellow, the S2 or S3 accelerograms which are characterized by the double wave effect do not subject the building to an increased demand than the S7 record.

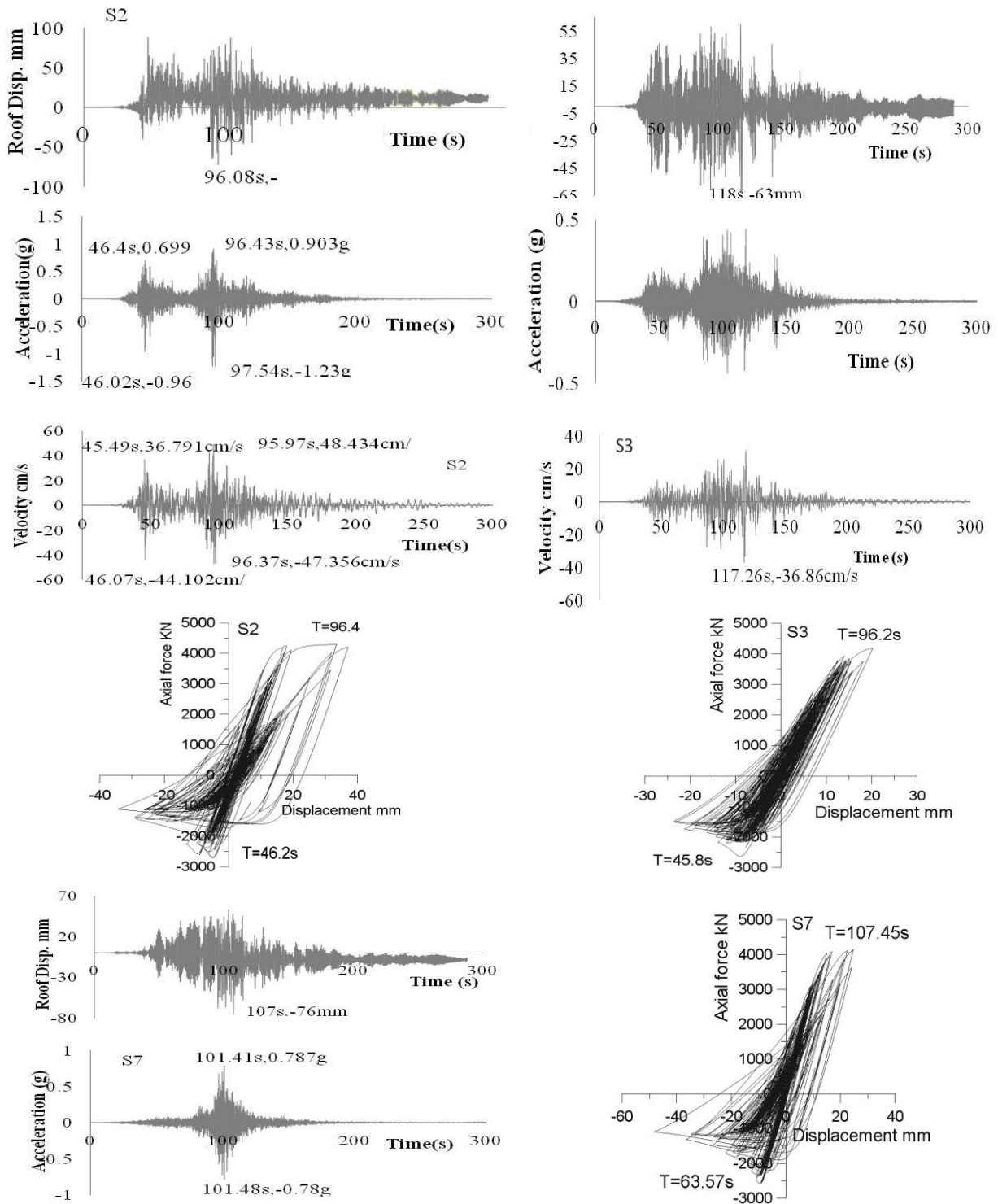


Figure 8. Seismic response of the 4-storey CBF building under S2, S3, and S7 ground motions.

4 Conclusions

The nonlinear behaviour of a 4-storey moderately ductile CBF building located in Victoria was analysed under two sets of ground motions: crustal and subduction. The CBF model was developed in the OpenSees environment and the investigated parameters are: interstorey drift, residual interstorey drift, and the type of failure mechanism. In this analysis, subduction ground motions were scaled with a factor of 1.0, while a computed scaling factor was applied to crustal ground motions.

- The low-rise building is prone to the formation of a ground floor storey-mechanism. The interstorey drift was accumulated within a floor (ground floor), where large tensile forces have been developed in braces after the occurrence of buckling. Braces of the floors above responded mostly in the elastic range. The interstorey drift of the upper floors was found to be lower than $0.8\%h_s$. However, the residual roof deformations were triggered under the C1 and C2 ground motions, as well as under the S1, S2 and S7.
- The long-duration subduction ground motions did not show a larger demand than the scaled crustal records, despite their large amplitudes of acceleration. However, in the short period range, ($T < 0.35$ s), the spectral acceleration ordinates were amplified by a factor larger than two. Thus, as the building is characterized by a fundamental period lower than 0.35 s, the exposure at seismic risk is high. The shape of subduction accelerograms that captured two adjacent seismic waves that arrived at a small time interval did not seem to have a special effect on the behaviour of the building.
- The plotted hysteresis loops show tensile failure of one of the two ground floor braces under C1 ground motion, while the same brace experienced initiation of tensile failure under the S2 record. However, caution may be applied when fatigue material is used.

Acknowledgements

Authors thank Prof. Gail Atkinson and Dr. Ghofrani for providing valuable input on the selection of subduction ground motions.

References

- Aguero.A., Izarnari.C., Tremblay. R. (2006). "Modeling of the Seismic Response of Concentricly Brace Steel Frames using the OpenSees Analysis Environment". *J. of Advanced Steel Constr.*, 2,3, 242-274.
- American Society of Civil Engineers (ASCE). (2005). "Minimum design loads for buildings and other Structures". *ASCE/SEI 7-05*, Reston, Virginia.
- Atkinson, G. and Macias, M. (2009). "Predicted ground motions for great interface earthquakes in the Cascadia subduction zone". *Bulletin of the Seismological Society of America*, v. 99, no.3, 1552-1578.
- Canadian Standard Association, CAN/CSA-S16 (2009). "Limit states design of steel structures". Toronto.
- De Luca, F., Chioccarelli, E., Iervolino, I. (2011). "Preliminary study of the 2011 Japan earthquake (M9.0) ground motion records V1.01". www.reluis.it.
- Ghofrani, H., Atkinson, G, Goda, K. (2012). "Implications of the 2011 M9.0 Tohoku Japan earthquake for the treatment of site effects in large earthquakes". *Bulletin Earthquake Engineering*.
- Earthquakes Canada (2012). www.earthquakescanada.nrcan.gc.ca.
- Hsiao, P.C., Lehman, D., Roeder, C. (2012). "Improved analytical model for special concentrically braced frames". *Journal of Constructional Steel Research*, 73:80-94.
- National Research Council of Canada (2010). National Building Code of Canada – Part 4, Ottawa, ON.
- Mazzoni, S., McKenna, F., Scott, M., Fenves, G. et al. (2007). "OpenSees User Manual".
- McKenna, F., Fenves, G.L. (2004). "Open System for Earthquake Engineering Simulation (OpenSees)", *PEER*, University of California, Berkeley, CA.
- Reyes, J.C. and Kalkan E. (2011). "Required number of records for ASCE/SEI 7 ground motion scaling procedure". *U.S. Geological Survey Open-File Report 2011-1083*, 34p.
- Strong-motion seismograph networks. (2012) www.k-net.bosai.go.jp, Japan.
- Uriz, P. (2005). "Towards earthquake resistant design of concentrically braced steel buildings". *Ph.D. Dissertation*, University of California, Berkeley.